ISSN 2075-1087, Gyroscopy and Navigation, 2024, Vol. 15, No.3, pp. 3-13.
Russian Text © The Author(s), 2024, published in Giroskopiya i Navigatsiya, 2024, No.3, pp. 3-20.

Analysis of Ring Laser Gyro Errors during Path Length Active Stabilization

S.A. Bolotnov[a], S.I. Nazarov[a] (ORCID: 0000-0002-2452-9457), A.O. Sinel'nikov[a, b, *] (ORCID: 0000-0002-5579-3509), N.V. Tikhmenev[a] and A.A. Ushanov[a] (ORCID: 0009-0009-3703-9981)

[a] *State Scientific Research Institute of Instrument Engineering (GosNIIP), Moscow, Russia*
[b] *People's Friendship University of Russia (RUDN University), Moscow, Russia*
**e-mail: mr.sinelnikov.a@mail.ru*

Received: January 28, 2024; reviewed: July 24, 2024; accepted: September 30, 2024

Abstract: The paper considers active stabilization of a ring laser gyro (RLG) path length in a wide range of temperatures, using a movable mirror with a piezoceramic drive. Analysis of the main designs of piezo actuators used in the RLG made in Russia is presented. Computer models of piezo actuators have been developed to study the distortions and curvatures of piezo-driven mirror surfaces based on their resonant oscillatory characteristics. By comparing the calculated data and the experimental results, a relationship between the movements of mirrors and the output parameters of RLG has been found. Possible improvements of piezo actuator structures are proposed, which make it possible to increase the accuracy and performance characteristics of RLG.

Keywords: ring laser gyroscope, piezo actuator, piezo-driven mirror, piezoelectric block, resonant oscillations, oscillation types, modes, total energy loss in resonator, diffraction loss, error model, path length control system.

1. INTRODUCTION

Currently, He-Ne ring laser gyroscopes (RLG) with a bias of 0.05-0.001 deg/h are mainly used as angular displacement sensors in autonomous inertial navigation systems [1–5] and short-term navigation systems. Although the early predictions were unfavorable, the scope of the RLG applications is continuously expanding [4, 6, 7]. The most important scientific results were obtained in the 1970s–1990s [8–11]; however, the research aimed at further improvement of the RLG accuracy and performance characteristics is still in progress, and some areas of research remain relevant [12–19].

Today leading manufacturers produce the RLG with accuracy of several thousandths of degree per hour. The RLG parameters and quality improvement has been achieved due to the enhanced technology, lower prime cost, and reduction of the overall dimensions of the ring laser resonator (RLR). The leading position here is occupied by Honeywell (USA) which provides the bias stability up to 0.003 deg/h in devices such as GG-1320 with a three-mirror resonator and with RLR length equal to 15.2 cm.

It is well known that the RLR length should be kept constant ($L = L_0 = \text{const}$) and divisible by the integer number of lasing waves, which is $\lambda = 0.633$ μm for a He-Ne laser [10]. This is provided by a path length control system with an actuating element consisting of one or two movable mirrors connected to a piezoceramic drive. The linear dimensions of the resonator can change under the effect of ambient temperature and the laser self-heating [20, 21]. The latter is caused by the DC glow discharge which maintains lasing, and by heat release from other electronic systems that support the RLG functioning [22, 23].

Figure 1 shows a diagram of thermal deformation of the axial contour of RLG with magneto-optical bias based on the Zeeman effect (Zeeman RLG) during active perimeter stabilization using movable mirrors [24].

As can be seen from Fig. 1, when the thermal expansion of the resonator is compensated with movable mirrors, the position of the optical resonator circuit changes relative to the membrane and the axes of the discharge channels. This leads to a change in the RLG bias magnitude due to the diffraction and Langmuir drifts [12, 22].

The bias of gas lasers can be caused by various physical phenomena [10–13, 22], but its stability mainly depends on the total loss in the resonator and the non-uniformity of the active medium gain [25]. These parameters, in turn, depend on the location of the optical circuit relative to the internal elements of the laser.

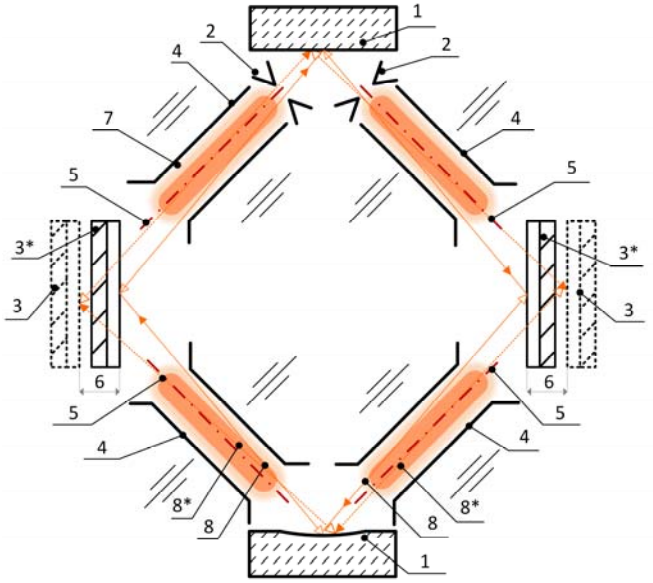

Fig. 1. Diagram of thermal deformation of the axial contour of Zeeman LG: 1 – fixed mirrors; 2 – membrane; 3 – movable mirrors before the resonator temperature change; 3* – displaced movable mirrors after the resonator temperature change; 4 – discharge channels; 5 – axes of discharge channels; 6 – displacements of movable mirrors w; 7 – active medium amplification zone; 8 – counter-propagating beams before the resonator temperature change; 8* – counter-propagating beams after the resonator temperature change.

When the RLR length is actively stabilized by moving the mirrors (3), the position of its axial circuit (8) changes relative to the center of the membranes (2) and the axes of the discharge channels (5), as a result of which the diffraction loss of the resonator changes and the active medium is amplified.

To minimize the above-mentioned displacements, the RLR housing [10, 11, 17, 26–28] is made of glass ceramics with the lowest coefficient of thermal expansion (CTE) [26–30]. To date, the CTE of the materials used is approaching the maximum achievable values [30] and its further qualitative reduction is not expected.

The RLR length change due to the temperature effects can be $L = L_0 \pm 3\lambda$ [29, 31]. This causes uncontrolled deformations of the resonator, as well as displacement and distortions of the reflective surfaces of the mirrors, which leads to the optical circuit misalignment. This problem can be aggravated by additional structural elements, as well as inhomogeneous temperature distribution within the cavity/resonator. Thus, the research in the field of piezo actuator geometry remains relevant [32, 33].

The researchers work on passive stabilization of the RLR length by introducing a mechanism to compensate for its thermal expansion into the piezo actuator design [34–36], in particular, to control the counter-deflection of the piezo-driven mirror membrane. Such thermally compensated systems reduce the control voltage and expand the total range of displacement of the movable mirror surfaces. Nevertheless, this does not solve the problem of deformations and distortions.

There are some known methods for calculating the axial circuit shift caused by the displacements and curvatures of mirrors [37, 38], and related diffraction loss and selection of resonator modes [38–40]. It is also known that the sensitivity of resonator losses to the mirror movements decreases as the beam is passing through the membrane center [38].

Thus, it remains relevant for laser gyroscopy to develop an engineering solution that provides precision (by units of nanometers) movement of the reflective surface of piezo-driven mirrors with no distortions and deflections leading to uncontrolled displacement of the RLR optical circuit. The search for such a solution should be based on the results of studies of existing piezo actuator designs as a whole, including the mirror substrate, piezoelectric actuator and their connection.

Within the framework of this work, recommendations have been developed to optimize the design of piezo actuators with the aim to improve the accuracy and performance of the RLG made in Russia.

The work contains the following main sections:

- analysis of the main designs of piezo actuators widely used in Russia;
- simulation of movement of piezo-driven mirror surfaces with active stabilization of the RLG path length;
- experimental studies of the amplitude-frequency response of piezo actuators;
- experimental study of the piezo actuator effect on RLG parameters;
- conclusions, including the discussion of results and practical recommendations.

2. ANALYSIS OF PIEZO ACTUATOR DESIGN FEATURES

Figure 2 shows two most common piezo actuator designs: PA1 and PA2 (*a* and *b*, respectively), which are used for path length active stabilization in the most common Russian-made RLG [14, 15].

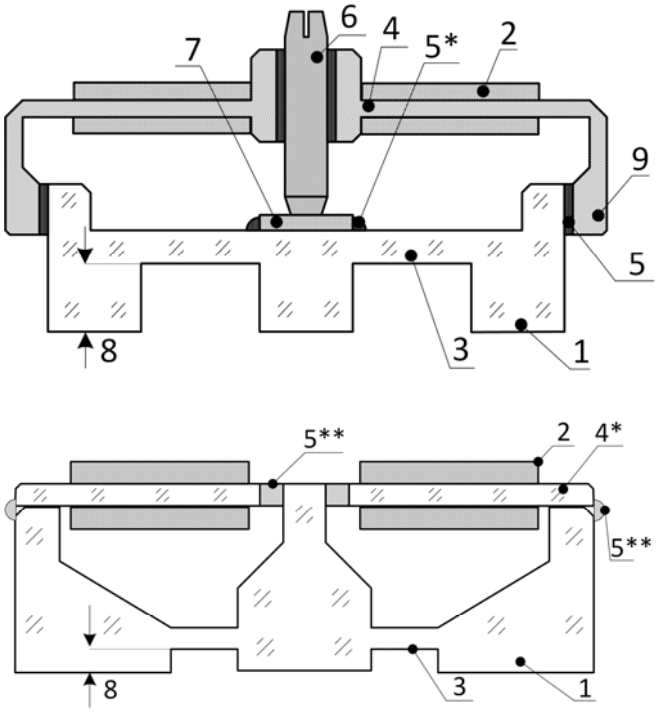

Fig. 2. Most common designs of Russia-made piezo actuators: *1* – mirror substrates; *2* – ring-shaped piezoelectric elements; *3* – deflecting membranes of piezo-driven mirrors; *4* – deflecting membranes (discs) of piezoelectric actuators (*4* – metal one, *4** – glass ceramic one); *5* – piezoelectric block and piezo-driven mirror joints (*5* – hard adhesive, *5** – soft adhesive, *5*** – soft soldering); *6* – pusher rotor creating the initial tension; *7* – metal disc transferring the force from the pusher rotor *6* to the membrane of piezo-driven mirror *4*; *8* – membrane depth *p*; *9* – clamp.

The PA1 version shown in Fig 2b is used in most of well-known international and Russian dither-mounted RLG [14]. All the joints shown in PA1 are made with hard epoxy adhesive. Further, in the computer model, these joints are assumed to be absolutely rigid, without taking into account the properties of the adhesive.

Figure 2b shows the PA2 used in the Zeeman RLG [15]. All the joints shown in PA2 are made with soft tin-lead solder. Softness or stiffness of the joint is estimated in comparison with the materials to be connected, namely glass ceramics such as optical ceramics SO-115M, from which the housing and mirrors of the RLR are made, and metals of the Invar H36 type, used in both designs of the piezo actuator.

The main difference between the piezo actuators under study is that PA1 always has a tense working position. As can be seen from Fig. 2a, the PA1 membrane bends due to the pushing force in the absence of forces acting in the opposite direction. The screw *6* creates constant deflection of the membrane *3* to ensure the reciprocating motion of the substrate of the movable mirror *1*, which is essential for the path length control system operation. In this case, the membrane remains stressed throughout the entire service life of the device. On the contrary, the design of the PA2 lets the mirror move in both directions and does not provide for constant elastic deformation of the membrane. Such an engineering solution is an obvious advantage of the PA2.

Another important feature of any piezo actuator design is different CTE of the mirror substrate and the piezoelectric block placed on it. In PA2, due to the difference in CTE of piezoceramic elements *2*, the piezoelectric block has a greater thermal expansion coefficient in the radial direction than the glass ceramic substrate of the piezo-driven mirror *1* [41]. To prevent this from leading to additional temperature-dependent curvature of the reflective surface of the mirror, flexible soldered joints *5** are used between the piezoelectric block and the mirror substrate. In PA1, the same effect is achieved due to the elasticity of longer clamps *9*.

3. SIMULATION OF PIEZO MIRRORS' REFLECTING SURFACE MOTION DURING ACTIVE STABILIZATION OF RLG PATH LENGTH

Let us consider the movement of the reflecting surfaces of piezo-driven mirrors with active stabilization of the RLG path length. This movement can be studied using three-dimensional models of the piezo actuator in the ANSYS software environment. As a result of modeling the piezo actuator and simulating its movements by the method of finite elements, it will be possible to detect the mirror surface deflection and calculate the change in this surface curvature radius R_l. In Fig. 3, the calculated values of the mirror surface curvature radius R_l depending on the depth of the membrane p are shown for PA2.

It can be seen that with a small depth of the membrane $p = 0.5$–1 mm, a change in the RLR path length by wavelength ($L = L_0 - \lambda$) leads to a change in R_l by up to 15%. With large depths of the membrane, this dependence disappears. Therefore, $p \geq 3$ mm is suffi-

cient for the reflecting surface to remain flat when the central part of the piezo-driven mirror is moving.

It is difficult to determine the magnitude of the distortions by calculation, since the asymmetry of the structure cannot be determined from design tolerances with acceptable reliability. One of the possible solutions is to study the design of piezo actuators using computer modeling of vibrational (resonance) characteristics. To this end, the eigen frequencies and forms of mechanical oscillations of both piezo actuator designs were calculated in the ANSYS software environment. Figures 4 and 5 show the types of oscillations (modes) and resonance frequencies of PA1 and PA2, respectively.

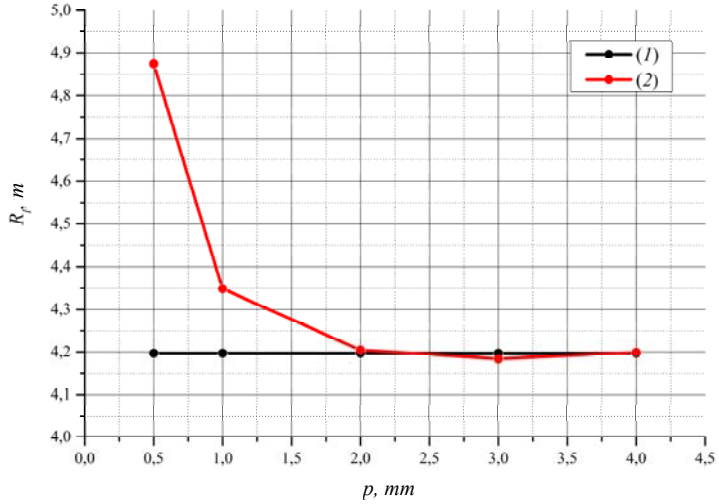

Fig. 3. Change in the radius of curvature of a spherical mirror: *1* – with a constant path length *($L = L_0 = const$)*; *2* – with the path length reduced by the wavelength value due to the piezo-driven mirror displacement ($L = L_0 - \lambda$)

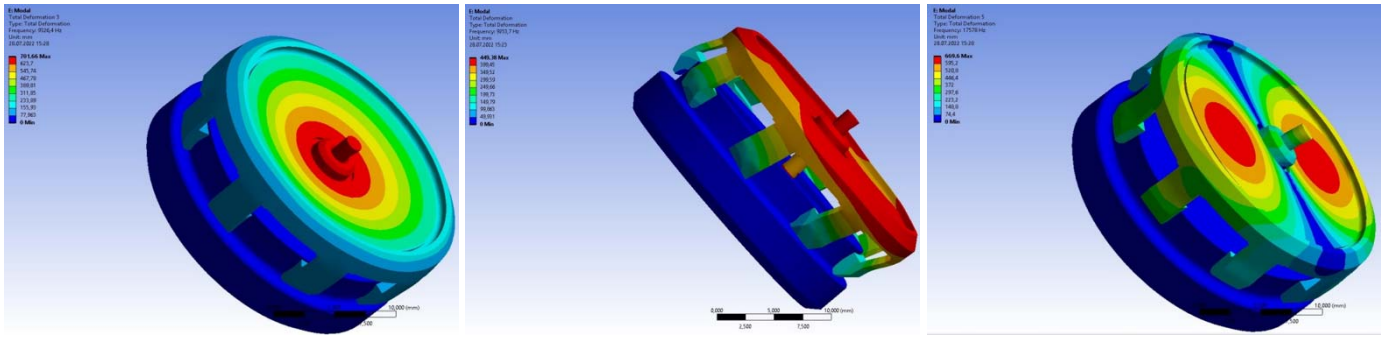

Fig. 4. Types of oscillations of PA1: *a*) $f = 9325$ Hz – reciprocating motion; the main even mode; *b*) $f = 9250$ Hz – lateral displacements of piezoelectric block due to the screw slip on the disc; parasitic modes; *c*) $f = 17600$ Hz – deflection of membranes without the screw displacement; parasitic odd modes.

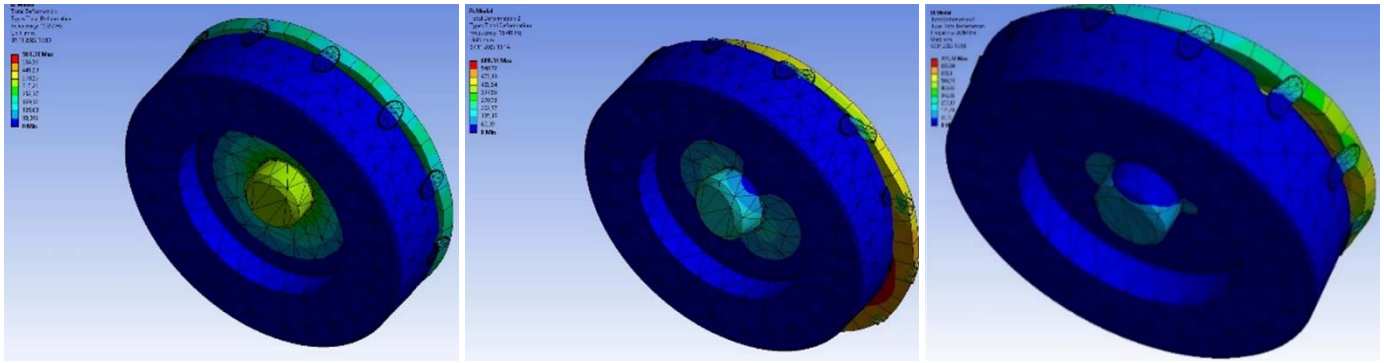

Fig. 5. Types of oscillations of PA2: *a*) $f = 15522$ Hz – reciprocating motion; basic even mode; *b*) $f = 16741$ Hz – deflection of membranes with piezoelectric block displacement; parasitic odd modes; *c*) $f = 20064$ Hz – deflection of membranes with piezoelectric block displacement and deflection: parasitic odd modes.

Figures 4a and 5a show the basic zero-order modes of both piezo actuators, which correspond to the reciprocating movement of the reflecting surface of the piezo-driven mirrors. With this type of movement, the path length L changes without any additional uncontrolled deformations of the optical circuit. Here we

consider only the deflection of membranes of the piezo-driven mirrors and piezoelectric block. The membrane depth is assumed to be large enough ($p > 3$ mm) so that the central part of the coated mirror does not deform (see Fig. 3). The direction of displacements of the reflecting surface of the mirror w occurring at these modes coincide with that of the driving force F generated by the piezo drive, which is a centrally symmetric even function similar to the delta function. When modeling the impact, the driving force F acts along the axis of the piezo actuator and has the form:

$$F(r=0) = F_0,\ F(r>0) = 0,$$

where r is the radius vector in the polar coordinate system with the origin in the geometric center of the piezo actuator.

The displacements of the mirror surface and both membranes at the main mode are also centrally symmetric even functions. Distortions of the central part of the mirror do not occur when such oscillations are excited. Figures 4b, 4c, 5b and 5c show the models of higher (first) order modes with an odd distribution of the membrane deflection, constructed in the ANSYS environment. The types of deflections in the one-dimensional version are schematically shown in Fig. 6.

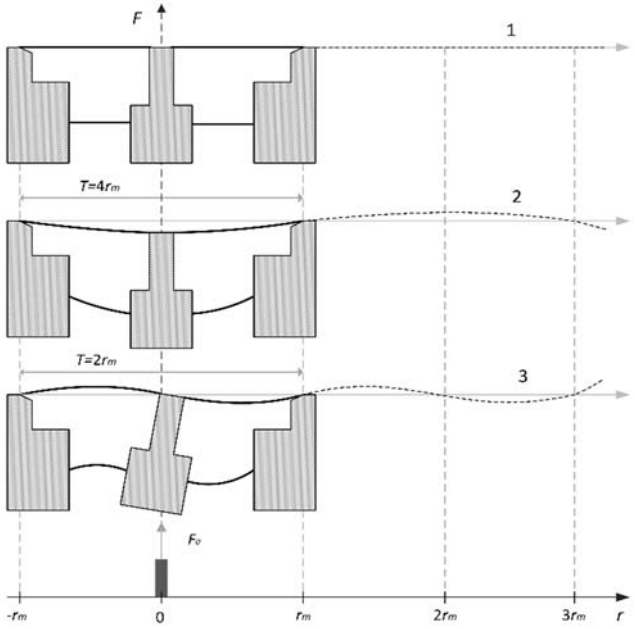

Fig. 6. Diagrams of piezoceramics oscillation types: *1* – undeformed (steady) state; *2* – the basic zero-order mode (even); *3* – the first-order mode (odd).

Membrane deflections are described by periodic functions with spatial periods $T = 2r_m$ for the zero mode and $T = r_m$ for the first-order mode, where r_m is the radius of the mirror. There is no sense to consider the modes of an order higher than the first one, since the distributions of their amplitudes at the point $r = 0$ (Fig. 6) repeat either the zero or the first-order modes.

As is known [42, 43], resonant oscillations can be excited when the frequencies of the acting force and the eigen frequency of oscillations (mode) coincide, as well as the spatial distribution of the effect and the amplitude of eigen oscillations. This phenomenon is clearly demonstrated in [43] and mathematically described by the integral of the product of the mode amplitude distributions and the driving force in the area of their interaction. This integral will be zero for odd oscillation modes and for the even driving force being considered, since these functions are orthogonal. Excitation of an odd mode is possible only if the parity of the driving force distribution function or the eigen mode oddness are violated.

In practice, both cases are possible. For example, when the screw which sets the initial tension of membranes in the piezo-driven mirror and piezoelectric block is shifted relative to the center of the PA1, the disk may get displaced relative to the center of the piezo-driven mirror, the adhesive connecting the piezoelectric block membrane and the piezoelectric elements may distribute non-uniformly, etc. For the described reasons, angular displacement of the reflecting surface of the mirror (skew) may happen not only during resonant oscillations, but also during slow displacements of the mirror surface under the pressure of the piezoelectric drive.

4. EXPERIMENTAL STUDIES OF PIEZO ACTUATOR FREQUENCY RESPONSE

Let us compare the calculation results for the resonance modes of piezo actuator operation, obtained by computer simulation methods, and their frequency response observed in the experiments.

A simple and informative method for determining the frequency response is as follows. The piezoelectric block contains two piezoceramic elements. One of them is supplied with alternating voltage U_1 from a frequency scanning generator, so the mechanical oscillations of the piezo actuator are created due to the reverse piezoelectric effect. Voltage U_2 proportional to the amplitude of mechanical oscillations of the piezo-driven mirror surface is recorded on the second piezoelectric element. It is possible to register the occurrence of the reflecting surface distortions by the presence of auxiliary resonance peaks in the frequency response curve. In the operating frequency range (up to ~20 kHz) of the piezo actuator,

there should be one resonance peak corresponding to the main zero mode. The peaks corresponding to even higher-order modes occur at frequencies above 30 kHz and are of no interest.

Figures 7a and 7b show the waveforms obtained experimentally for PA1 and PA2, respectively. Frequency response measurements were taken for several samples of both types of piezo actuators. Most of PA2 samples had a single pronounced peak, and the frequency response had weak distortions in the form of auxiliary peaks with a magnitude not exceeding 5-7% of the maximum value of the main mode. Frequency response of PA1 in all cases contained one or two auxiliary peaks with amplitudes comparable to the main mode peak amplitude. The table shows the measured values of the resonance frequencies f and relative amplitudes A of the first three modes of PA1. It can be seen that the relative amplitude A_{10} of the satellite mode reached 75% (sample no. 5).

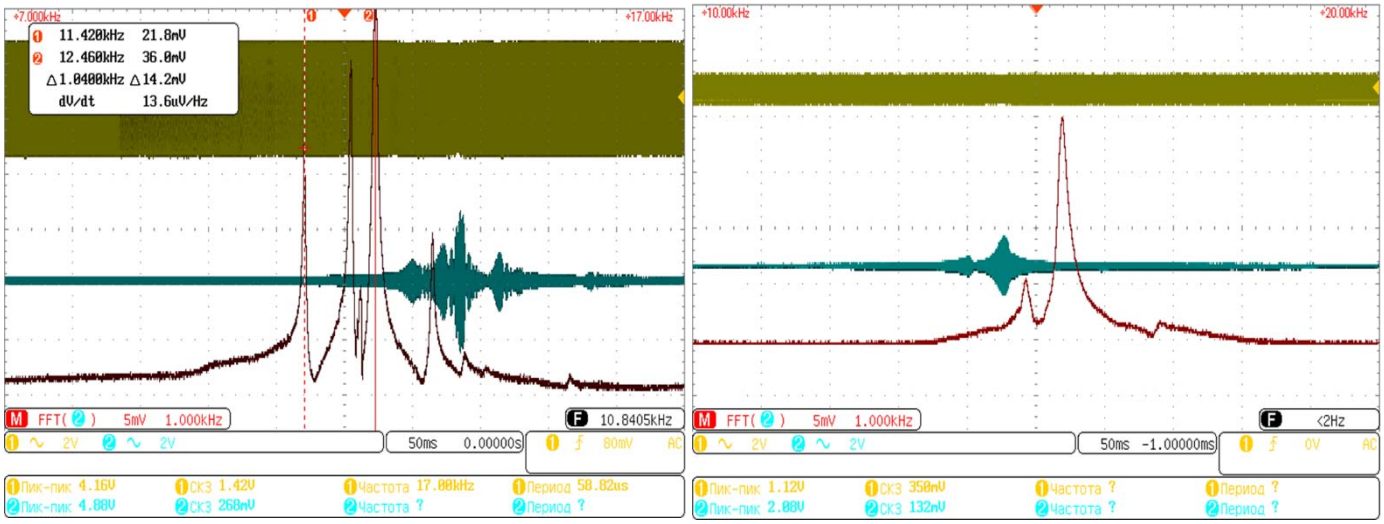

Fig. 7. Frequency response waveforms of piezo actuators: *a*) waveform typical of PA1; *b*) waveform typical of PA2.

Table 1. Resonance frequencies of piezo actuators' eigen oscillations

PA1 no.	Resonance frequencies f, KHz			Relative amplitude A, %		
	f_{01}	f_{10}	f_{00}	A_{01}	A_{10}	A_{00}
1	–	11.62	12.04	–	52.69	100.00
2	11.33	11.67	12.00	43.95	43.15	100.00
3	11.41	12.09	12.45	45.29	68.24	100.00
4	11.42	12.09	12.46	27.78	61.11	100.00
5	11.60	12.50	12.97	21.67	76.39	100.00
6	11.62	12.53	12.95	8.36	54.33	100.00

Studies of piezo actuator designs show that it is important to properly select and optimize almost all geometric dimensions of this device [33–36]. High probability of distortions in PA1 is caused by the presence of extended elastic clamps shown in Fig. 2a [36]. In this design, the piezoelectric block shifts laterally relative to the piezo-driven mirror substrate, and this leads to displacement of the contact point of the pushing screw relative to the center of the piezo-driven mirror (asymmetry of the driving force F), and skew of the reflecting surface. This displacement is limited only by the friction between the central screw and the central metal disc. Computer simulation and the results of experiments show that when the friction coefficient is about 0.1-0.3, the calculated resonance frequency of the satellite modes proves to be less than the frequency of the main type of oscillations.

The distortion of the mirror's reflecting surface leads to the displacements of the axial circuit of the RLR, change in the laser beam position relative to the membrane axis and, consequently, change in diffraction losses. The change in the resonator losses affects the gain level and the lasing intensity I. Typical dependences of the ring laser radiation intensity when changing the path length $I(L)$ by setting the control voltage of the piezoelectric drive are shown in Fig. 8.

It should be noted that the dependences $I(L)$ for different laser samples differ significantly and in a random way. In addition, the intensity can both decrease and increase when the mirror is moving in one direction, for example, inside the RLR.

It is known [38–40] that the extent of diffraction loss dependence on the beam displacement along the membrane is associated with the initial position of the

beam relative to the membrane center; in other words, it depends on the accuracy of the resonator alignment. The higher the initial diffraction losses, the greater the change in these losses will be with the same displacement of the beam along the membrane. The distortions can vary significantly for each particular piezo actuator sample. Consequently, the losses in the RLR depend on two factors: the accuracy of alignment and the distortions of the mirror. If any of these is eliminated, the accuracy characteristics of the RLG, including the bias stability, will improve. The method of alignment and its accuracy depend on the technology [44–46], and no noticeable improvement is expected here. Therefore, the reduction of distortions and deformations of the piezo-driven mirror is a key factor in improving the RLG accuracy.

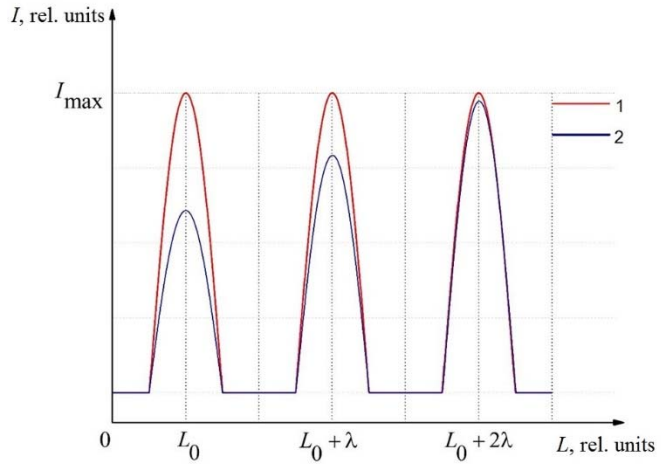

Fig. 8. Dependence of the output radiation intensity of ring laser on the change in the piezo actuator path length: *1* – weak dependence of the intensity on the piezo actuator scanning; 2 –strong dependence of intensity on PA2 scanning.

In PA2, piezoelectric block expansion is compensated by elastic deformation of the soft solder. Thus, the design is simplified and the mirror center distortions caused by imperfect symmetry of the piezoelectric block are eliminated. In addition, the PA2 design ensures that the piezoelectric block is centered relative to the mirror without any potential lateral shifts, with accurate reference of the point of force F application to the geometric center of the piezo-driven mirror.

Calculation of the computer model resonances shows that there are no low-frequency oscillations when using the solder with characteristics corresponding to the real material used in the PA2 design. In this case, distortions are unlikely, which is also confirmed by experimental studies of frequency response and the results of independent works. In particular, in [32] it was experimentally shown on a large number of mirror samples that the angular distortions of PA2 do not exceed 3.5 arc sec.

5. EXPERIMENTAL STUDY OF THE EFFECT OF PIEZO ACTUATORS ON RLG PARAMETERS

Let us consider the effect of piezo actuator operation on the parameters of light generation in a ring laser by example of the Zeeman RLG. Due to the specific features of the physical optical circuit [8, 15], the Zeeman RLG is a convenient tool for fundamental research with the possibility of precision control of changes in the ring laser optical resonator losses by the frequency of Zeeman beats Δf [16, 50]. In dither-mounted RLG, the accuracy of such control of radiation intensity losses is significantly lower.

It was found experimentally that the loss reduction on all samples of the Zeeman RLG is always associated with the same direction of the mirror movement. When the mirror moves outward and the membrane deflects towards the piezoelectric block (Fig. 1), which corresponds to the pulling force of the piezoelectric drive, the losses decreased, and the radiation intensity increased (Fig. 8, plot 2). On the other hand, the loss increased with the pushing force of the piezoelectric drive, i.e., when the mirror deflected into the resonator. The loss function of the resonator is related to the mirror reflecting surface deformation under the action of the piezoelectric drive. Obviously, the pulling motion of the piezoelectric drive reduces the radius R_l of the mirror curvature, while the pushing motion leads to its increase. Based on the above computer model, one can calculate the changes in the parameters depending on the changes in the spherical mirror curvature radius (Fig. 3).

The ring laser alignment is carried out by the multipath interference method as described in [44–46]. The quality of mirrors and the accuracy of RLR housings determine the total energy loss and relative selectivity C_s of the transverse electromagnetic modes (TEM) (differing both in frequency and intensity of distribution in the Gaussian beam) according to the following relationship:

$$C_s = (\sigma_{01} - \sigma_{00}) / \sigma_{00}, \quad (1)$$

where σ_{00} is the loss of the resonator on the main mode TEM_{00}, $\sigma_{01} = \sigma_{10}$ is the loss of the resonator on the first transverse modes TEM_{01} and TEM_{10} (identical in a nonplanar resonator of the Zeeman RLG [31].

The degree of dependence of the characteristic describing the level of diffraction loss α on the membrane diameter d increases rapidly [38–40] with decreasing geometric dimensions of the mem-

brane relative to the diameter of the Gaussian beam or with increasing diameter of the beam with the membrane size being constant. The dependence $\alpha(d)$ for a fixed curvature radius R_l of spherical mirror in a symmetric nonplanar resonator of Zeeman RLG is shown in Fig. 9.

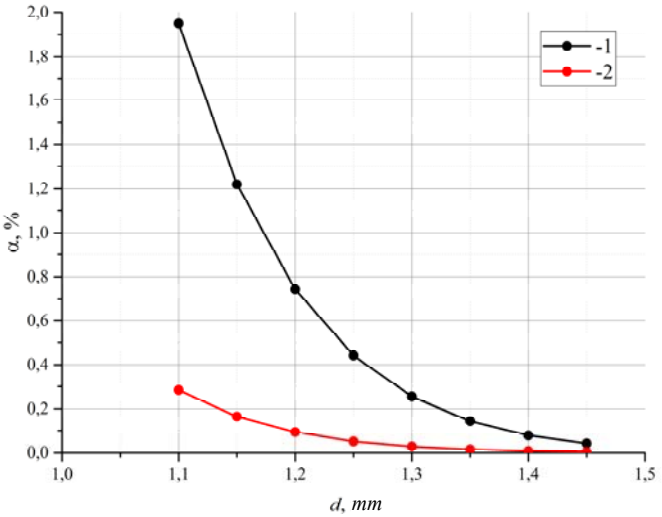

Fig. 9. Dependence of diffraction loss on the membrane diameter: *1* – loss on the mode TEM_{01}; *2* – loss on the mode TEM_{00}.

It can be seen in Fig. 9 that the increase of α at fixed d is associated with the difference in losses Δα between the modes TEM_{01} and TEM_{00} or the relative selectivity C_s. This feature can be used in the experiments to determine the diffraction loss α in the RLR [49, 50]. Calculated dependence of the diffraction loss α_{00} on the main mode TEM_{00} on Δα is shown in Fig. 10. The line in this figure shows the empirical approximating curve 2 described by the formula

$$\alpha_{00} = 0.125\cdot(\sigma_{01} - \sigma_{00}) + 0{,}03\cdot(\sigma_{01} - \sigma_{00})\cdot(\sigma_{01} - \sigma_{00}). \quad (2)$$

Figure 11 presents the experimental results demonstrating the relationship between the sum of losses l_{mir} of the mirrors, measured on the mirrors before they were installed in the resonator, and the loss of resonators σ_{00} minus the diffraction loss α_{00}. In fact, these are the same characteristics, and their coincidence confirms the reliability of the method of their measurement and calculation ($l_{mir} \approx \sigma_{00} - \alpha_{00}$). As can be seen in Fig. 11, the experimental points are concentrated around the asymptote with a single slope, which indicates the coincidence of measured values and confirms the method validity.

We calculate the loss σ_{00} and the frequency of Zeeman beats Δf depending on the change of the ring laser path length for piezo-driven mirrors with a small depth of membrane p = 1 mm, taking into account the quality of alignment. Using a computer model, we calculate the change in the curvature R_l of the reflecting surface of a spherical mirror. After that, knowing the typical passive losses of resonators (about 0.3%) and setting the extreme values of selectivity ($C_s = min$, $C_s = max$), we find the diffraction loss α_{00} and the total loss of the resonator σ_{00}. Then we determine the frequency of the Zeeman beats Δf depending on the path length L from the total loss of the resonator σ_{00} for the two extreme values of selectivity C_s.

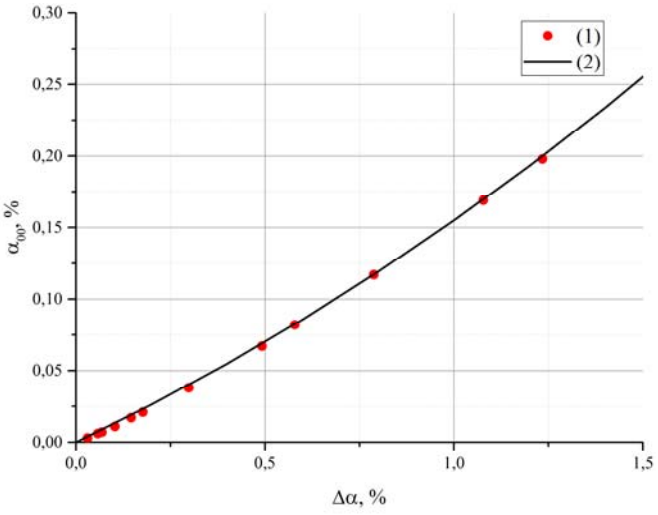

Fig. 10. Dependence of diffraction loss on the difference between the losses on modes TEM_{01} and TEM_{00}: *1* – theoretical dependence; *2* – approximating function.

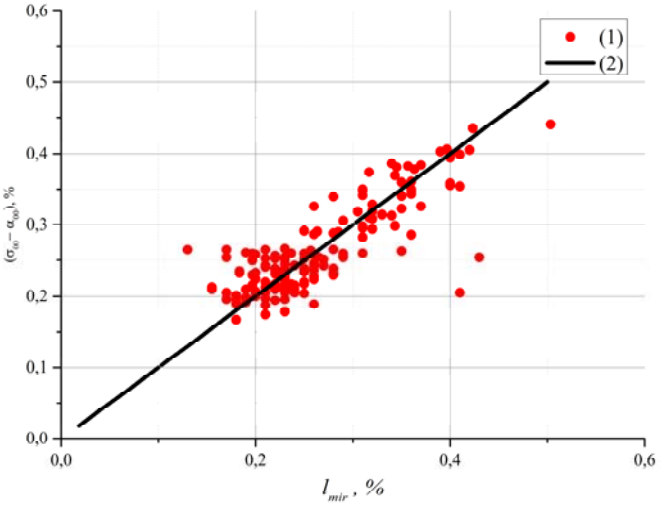

Fig. 11. Relationship between the sum of mirror losses and resonator losses minus diffraction losses: *1* – experimental measurements; *2* – approximation.

Theoretical plots of Δf (1 and 2) are represented in Fig. 12 as solid lines. Plot 2 with lower values and smaller slope angle corresponds to the minimum selectivity ($C_s = min$, p = 1 mm), and plot 1 with a larger slope angle corresponds to the maximum selectivity ($C_s = max$, p = 1 mm).

The frequencies of Zeeman beats Δf correspond to longitudinal modes with the same type of polarization

and uniquely characterize the resonator losses on a mode with corresponding longitudinal index. Dotted lines show the experimental dependencies of Δf 3–6 for the longitudinal modes of various RLR. Their difference is associated with the accuracy of the optical RLR alignment and the technological spread of mirror losses l_{mir}. As expected, the experimental results for Δf lie within the calculated range and demonstrate a good agreement between the theory and experiment.

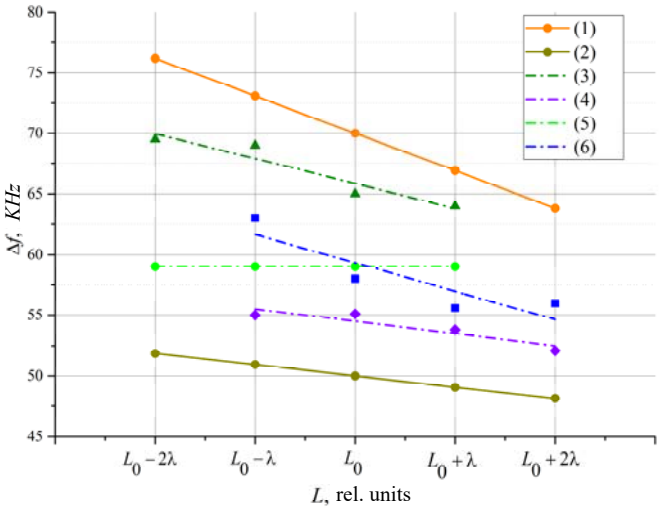

Fig. 12. Dependence of the frequency of Zeeman beats in a RLG (proportional to the resonator losses) in case of the ring laser path length change.

Based on the simulation results presented in Fig. 3, it was shown that the deepening the piezo-driven mirror membrane by an amount up to $p = 3$ mm makes it possible to avoid a change in the reflecting surface curvature radius R_l. To confirm these results, a model of PA2 was made with the mirror membrane depth of $p = 3$ mm. Plot 5 in Fig. 12 shows the dependence of the Zeeman beat frequency Δf on the size of the resonator for the PA2 design with $p = 3$ mm. Experimental dependence 5 is typical of all samples of such gyroscopes. It is not affected by changes in selectivity ($C_s = var$) and the size of the RLR.

Thus, the design of the PA2 with a greater depth of the membrane makes it possible to make the resonator losses σ_{00} independent of the piezo-driven mirror movement w within the permissible limits of the resonator parameters (l_{mir} and C_s). Comparison of experimental and theoretical dependencies in Fig. 12 confirms the conclusions of the research and proves that the piezo-driven mirror's reflective surface has no significant distortions in PA2.

6. CONCLUSION

The main known designs of RLG piezo actuators have been analyzed in terms of their resistance to distortions and deformations of the reflective surfaces of mirrors during reciprocating motion under the action of a piezoelectric drive performed to actively stabilize the ring laser path length in the range of external temperature variations.

Computer models of piezo actuators have been constructed, and the possibility of studying the distortions and deformations of piezo-driven mirror surfaces by their frequency response has been shown.

It has been found that the changes in the RLR internal losses are associated with distortions and deformations of the reflective surfaces of piezo-driven mirrors and lead to the RLG bias instability.

As a result of the study, it can be concluded that the instability of light intensity in dither-mounted RLG with PA1 is caused solely by the distortions of the mirror reflective surfaces, which occur when the piezoelectric drive force application point deviates from the center of elasticity of the piezo-driven mirror. To eliminate this effect, it is proposed to correct the location of the screw and disc relative to the center of the piezo-driven mirror. In addition, measures are needed to prevent the screw from slipping on the disc. There are also other recommendations for improving the PA1, e.g., to shorten the clamps or to solder the piezoelectric block to the mirror.

For PA2 used in the Zeeman and other types of RLG, the bending membrane which ensures the piezo-driven mirror mobility should have a depth of at least 3 mm relative to its surface.

The recommendations proposed in the work will make it possible to increase the RLG immunity to thermal and mechanical impacts without changing the RLR design.

FUNDING

This work was supported by ongoing institutional funding. No additional grants to carry out or direct this particular research were obtained.

CONFLICT OF INTEREST

The authors of this work declare that they have no conflicts of interest.

REFERENCES

1. Robin, L., Perlmutter, M., Gyroscopes and IMUs for Defence Aerospace and Industrial, Report by Yole Development, 2012.

2. Passaro, V.M.N., Cuccovillo, A., Vaiani, L., De Carlo, M., and Campanella, C.E., Gyroscope technology and applications: A review in the industrial perspective, Sensors, 2017, vol. 17(10), p. 2284, DOI: 10.3390/s17102284.
3. Rivkin, B.S., Analiticheskii obzor sostoyaniya issledovanii i razrabotok v oblasti navigatsii za rubezhom (Analytical Review of International Research and Developments in Navigation), vol. 6, St. Petersburg: Concern CSRI Elektropribor, JSC, 2021.
4. Damianos, D., Girardin, G., High-End Inertial Sensors for Defense, Aerospace & Industrial Applications, Market and Technology Report by Yole Development, 2020.
5. Peshekhonov V.G., The outlook for gyroscopy, Gyroscopy and Navigation, 2020, vol. 11, no. 3, pp. 193–197. https://doi.org/10.1134/S2075108720030062
6. Afanas'ev, V.B., Mamaev, V.A., Medvedev, V.M., Ostapenko, S.N., and Tikhmenev, N.V., On the issues of quality and reliability of laser inertial systems, Izv. Rossiiskoi akademii raketnykh i artilleriiskikh nauk, 2023, vol. 126, no. 1, pp. 87–95.
7. Wang, S., Zhang, Z., Research on principle, application and development trend of laser gyro, Journal of Physics: Conference Series, 2020, vol. 1549, no. 2, p. 022118.
8. Zeiger, S.G., Klimontovich, Yu.L., Landa, P.S., Lariontsev, E.G., and Fradkin, E.E., Volnovye i fluktuatsionnye protsessy v lazerakh (Wave and Fluctuation Processes in Lazers), Klimontovich, Yu.L., Ed., Moscow: Glavnoe izdatel'stvo fiz.-mat. literatury, 1974.
9. Bychkov, S.I., Luk'yanov, D.P., and Bakalyar, A.I., Lazernyi giroskop (The Laser Gyroscope), Moscow: Sovetskoe radio, 1975.
10. Aronowitz, F., Fundamentals of the ring laser gyro, in: Optical Gyros and Their Application, Loukianov D., Rodloff R., Sorg H., Stieler B., eds., RTO AGARDograph, 1999, vol. 339, pp. 3-1–3-45.
11. Lukyanov, D., Filatov, Yu., Golyaev, Yu., Kuryatov, V., Solovieva, T., Vasiliev, V., Buzanov, V., Spectorenko, V., Klochko, O., Vinogradov, V., Schreiber, K.-U., and Perlmutter, M., 50th anniversary of the laser gyro, Proc. 20th Saint-Petersburg International Conference on Integrated Navigation Systems, 2013, pp. 36–49.
12. Kravtsov, N.V., Kravtsov, N.N., Nonreciprocal effects in ring lasers, Quantum Electronics, 1999, vol. 29, no. 5, pp. 378–399. DOI: 10.1070/QE1999v029n05ABEH001495
13. Dao, H.N., Klimakov, V.V., Molchanov, A.V., and Chirkin, M.V. Gas dynamics in active medium and bias instability of laser gyroscope, Vestnik RGRTU, 2017, #59, pp.136–144. DOI:10.21667/1995-4565-2017-59-1-136-144
14. Kuznetsov, A.G., Molchanov, A.V., Chirkin, M.V., Izmailov, E.A., Precise laser gyroscope for autonomous inertial navigation, Quantum Electronics, 2015, vol. 45, no. 1, pp. 78–88. DOI: 10.1070/QE2015v045n01ABEH015420
15. Azarova, V.V., Golyaev, Yu.D., and Savel'ev, I.I., Zeeman laser gyroscopes, Quantum Electronics, 2015, vol. 45, no. 2, pp. 171–179. DOI: 10.1070/QE2015v045n02ABEH015539
16. Molchanov, A.V., Ring resonator geometric parameters in laser gyro errors estimation, Navigatsiya i upravlenie letatel'nymi apparatami, 2023, vol. 40, no. 1, pp. 37–64.
17. Chopra, K.N., Ring Laser Gyroscopes. Optoelectronic Gyroscopes. Progress in Optical Science and Photonics, Singapore: Springer, 2021, https://doi.org/10.1007/978-981-15-8380-3_1.
18. Tikhmenev, N.V., Nazarov, S.I., Ushanov, A.A., and Sinel'nikov, A.O., Study of the ring laser gyroscope functioning under vibration, Upravlenie bol'shimi sistemami, 2024, no. 109, pp. 293–309. DOI: 10.25728/ubs.2024.109.13
19. Weng, J., Bian, X., Kou, K., and Lian, T., Optimization of ring laser gyroscope bias compensation algorithm in variable temperature environment, Sensors, 2020, vol. 20(2), p. 377, https://doi.org/10.3390/s20020377.
20. Kuznetsov, E., Golyaev, Yu., Kolbas, Yu., Kofanov, Yu., Kuznetsov, N., Vinokurov, Yu., Soloveva, T., Thermal computer modeling of laser gyros at the design stage: a promising way to improve their quality and increase the economic efficiency of their development and production, Optical and Quantum Electronics, 2021, vol. 53(10), p. 596. https://doi.org/10.1007/s11082-021-03253-8
21. Zubarev, Y.A., Sinelnikov, A.O., Fetisova, N.E., A study of the temperature stability of the Zeeman laser gyro ring resonator, Proc. 29th Saint Petersburg International Conference on Integrated Navigation Systems (ICINS), 2022, pp. 1–4, https://doi.org/10.23919/ICINS51784.2022.9815336.
22. Sinel'nikov, A.O., Medvedev, A.A., Golyaev, Yu.D., Grushin, M.E., and Chekalov, D.I., Thermal zero drifts in magneto-optical Zeeman laser gyroscopes, Gyroscopy and Navigation, 2022, vol. 12, no. 1, pp. 308–313. https://doi.org/10.1134/S2075108721040076
23. Li, Y., Fu, L., Wang, L., He, L., Li, D., Laser gyro temperature error compensation method based on NARX neural network embedded into extended Kalman filter, in: Advances in Guidance, Navigation and Control. Lecture Notes in Electrical Engineering, Yan, L., Duan, H., Yu, X. (eds), vol 644, pp. 3309–3320, Springer, Singapore. https://doi.org/10.1007/978-981-15-8155-7_276
24. Sinelnikov, A., Kuznetsov, E., Golyaev, Yu., Kolbas, Yu., and Solov'eva, T., Computer simulation of the Zeeman laser gyros resonator length control system behavior, Proc. SPIE 12480, Optical Technology and Measurement for Industrial Applications Conference 2022, p. 1248002. https://doi.org/10.1117/12.2657469
25. Azarova, V.V., Golyaev, Yu.D., and Kuznetsov, E.V., Effect of unequal intensities of counter-propagating waves on the frequency response of laser gyroscopes, Gyroscopy and Navigation, 2020, vol. 11, no. 4, pp. 285–292. DOI: 10.17285/0869-7035.0050.
26. Sinel'nikov, A.O., Zapotyl'ko, N.R., Zubarev, Ya.A., and Katkov, A.A., Aspects of sitall SO-115M use in the fabrication of the optical components of He-Ne ring lasers, Glass and Ceramics, 2023, vol. 80, nos. 5–6, pp. 171–177. DOI 10.1007/s10717-023-00579-5
27. Naumov, A.S., Sigaev, V.N., Transparent lithium-aluminium-silicate glass-ceramics (Overview), Glass and Ceramics, 2024, vol. 80, nos. 11–12, pp. 491–499. DOI: 10.1007/s10717-024-00639-4
28. Naumov, A.S., Alekseev, R.O., Savinkov, V.I., and Sigaev, V.N., Crystal nucleation and growth in Li2O–Al2O3–SiO2 base glass bulk, Glass and Ceramics, 2023, vol. 80, nos. 7–8, pp. 307–312. DOI 10.1007/s10717-023-00604-7

29. Zubarev, Ya.A., Sinel'nikov, A.O., and Mnatsakanyan, V.U., Simulation of the temperature drift of the lase gyroscope path length, RUDN Journal of Engineering Research, 2023, vol. 24, no. 1, pp. 30–39. DOI: 10.22363/2312-8143-2023-24-1-30-39.
30. Sigaev, V.N., Savinkov, V.I., Shakhgil'dyan, G.Yu., Naumov, A.S., Lotarev, S.V., Klimenko, N.N., Golubev, N.V., and Presnyakov, M.Yu., On the possibility of precision control of the linear thermal expansion coefficient of transparent lithium-aluminum-silicate sitals near zero values, Glass and Ceramics, 2020, vol. 76, nos. 11–12, pp. 446–450. DOI: 10.1007/s10717-020-00220-9
31. Golyaev, Yu.D., Zapotyl'ko, N.R., Nedzvetskaya, A.A., and Sinel'nikov, A.O., Thermally stable optical cavities for Zeeman laser gyroscopes, Optics and Spectroscopy, 2012, vol. 113, no. 2, pp. 227–229. DOI: 10.1134/S0030400X12070090
32. Sukhov, E.V., Zapotyl'ko, N.R., Dependence of the shape and angle of the reflecting surface of mirror piezocorrector on the control voltage, Sbornik dokladov Rossiiskoi nauchno-tekhnicheskoi konferentsii s mezhdunarodnym uchastiem "Innovatsionnye tekhnologii v elektronike i priborostroenii" (Proc. Russian Scientific and Technical Conference with International Participation "Innovative Technologies in Electronics and Instrument Engineering"), Moscow: MIREA – Russian Technological University, 2021, vol. 1, pp. 293–296.
33. Ma, Y., Quan, B., Han, Z., and Wang, J., Structural optimization of the length control mirror for ring laser gyro, Proc. Second International Conference on Photonics and Optical Engineering, Xi'an, China, 2017, vol. 10256. DOI: 10.1117/12.2256501
34. Zapotyl'ko, N.R., Katkov, A.A., and Nedzvedskaya, A.A., Piezo actuator for compensating the thermal variations of the optical path length of the cavity of a laser gyroscope, Journal of Optical Technology, 2011, vol. 78, no. 10, pp. 644–645. DOI: 10.1364/JOT.78.000644
35. Zapotyl'ko, N.R., Katkov, A.A., and Sinel'nikov, A.O., Passive thermal compensation of the optical path length of laser gyros made from different constructional materials, Datchiki i sistemy, 2014, vol. 176, no. 1, pp. 8–13.
36. Borisov, M.V., Chernomorskii, A.N., and Chirkin, M.V., Choice of parameters of a ring cavity path length control device of a small-sized laser gyroscope, Aviakosmicheskoe priborostroenie, 2015, no. 11, pp. 13–20.
37. Ishchenko, E.F., Deformations of axial contour of optical resonator, Journal of Applied Spectroscopy, 1969, vol. 11, no. 3, pp. 1044–1049. https://doi.org/10.1007/BF00607840
38. Ishchenko, E.F., Otkrytye opticheskie rezonatory: Nekotorye voprosy teorii i rascheta (Open Optical Resonators: Selected Theoretical and Calculation Issues), Moscow: Sovetskoe radio, 1980.
39. Anan'ev, Yu.A., Opticheskie rezonatory i lazernye puchki (Optical Resonators and Laser Beams), Moscow: Nauka, 1990.
40. Bykov, V.P., Silichev, O.O., Lazernye rezonatory (Laser Resonators), Moscow: FIZMATLIT, 2003.
41. Vlasov, A.V., Zapotyl'ko, N.R., Katkov, A.A., et al., On the matter of technology for producing piezoelectric materials for laser gyros by cold uniaxial pressing and sintering, Polzunovskiy vestnik, 2022, no. 2, pp. 129–138. DOI: 10.25712/ASTU.2072-8921.2022.02.018
42. Pippard, A.B., The Physics of Vibration, Cambridge University Press, 1978.
43. Kogelnik. H., Coupling and conversion coefficients for optical modes, Proc. Symposium on Quasi-optics, New York, NY, June 1964, Brooklin, N.Y.: Polytechnic Press, 1964, pp. 210–225.
44. Heard, H.G., Laser Parameter Measurements, John Wiley & Sons, 1968.
45. Fedorov, A.E., Zborovskii, V.A., Rekunov, D.A., et al., Mirror adjustment and laser gyroscope resonator loss measurement, Proc. 22nd Saint Petersburg International Conference on Integrated Navigation Systems (ICINS), 2015, pp. 347–352.
46. Azarova, V.V., Bessonov, A.S., Bondarev, A.L., Makeev, A.P., and Petrukhin, E.A., Two-channel method for measuring losses in an optical ring resonator at a wavelength of 632.8 nm, Quantum Electronics, 2016, vol. 46, no. 7, pp. 650–654. DOI: 10.1070/QEL16008
47. Khromykh, A.M., Yakushev, A.I., Influence of resonance radiation trapping on the Zeeman effect in a ring laser, Soviet Journal of Quantum Electronics, 1977, vol. 7, no. 1, pp. 13–17. DOI: 10.1070/QE1977v007n01ABEH008389
48. Savel'ev, I.I., Khromykh, A.M., Longitudinal modes of a cavity ring laser, Soviet Journal of Quantum Electronics, 1976, vol. 6, no. 7, pp. 821–826. DOI: 10.1070/QE1976v006n07ABEH011681
49. Tikhmenev, N., Korshunov, S., Bannikov, D., and Protsenko, I., Measurement of losses of precision mirrors of ring lasers, Proc. 29th Saint Petersburg International Conference on Integrated Navigation Systems (ICINS), 2022, pp. 1–3. DOI: 10.23919/ICINS51784.2022.9815346
50. Korshunov, S., Tikhmenev, N., Bannikov, D., and Protsenko, I., Measurement of losses of precision mirrors of ring lasers, Proc. 29th St. Petersburg International Conference on Integrated Navigation Systems (ICINS), 2022. DOI: 10.23919/ICINS51784.2022.9815346.